Control of Adipocyte Thermogenesis and Lipogenesis through γ3-Adrenergic and Thyroid Hormone Signal Integration

Adilson Guilherme[1,*], Batuhan Yenilmez[1,4], Alexander H. Bedard[1,4], Felipe Henriques[1,4], Dianxin Liu[2,4], Alexandra Lee[1], Lauren Goldstein[1], Mark Kelly[1], Sarah M. Nicoloro[1], Min Chen[3], Lee Weinstein[3], Sheila Collins[2], Michael P. Czech[1,5,*]

[1]Program in Molecular Medicine, University of Massachusetts Medical School, Worcester, MA 01605, USA

[2]Departments of Medicine, Cardiovascular Medicine, and Molecular Physiology & Biophysics, Vanderbilt University Medical Center, Nashville, TN 37232, USA

[3]Metabolic Diseases Branch, NIDDK, NIH, Bethesda, MD 20892-1752, USA

[4]These authors contributed equally

[5]Lead Contact

SUMMARY

Here, we show that β adrenergic signaling coordinately upregulates *de novo* lipogenesis (DNL) and thermogenesis in subcutaneous white adipose tissue (sWAT), and both effects are blocked in mice lacking the cAMP-generating G protein-coupled receptor Gs (Adipo-GsαKO) in adipocytes. However, UCP1 expression but not DNL activation requires rapamycin-sensitive mTORC1. Furthermore, β3-adrenergic agonist CL316243 readily upregulates thermogenic but not lipogenic genes in cultured adipocytes, indicating that additional regulators must operate on DNL in sWAT *in vivo*. We identify one such factor as thyroid hormone T3, which is elevated locally by adrenergic signaling. T3 administration to wild-type mice enhances both thermogenesis and DNL in sWAT. Mechanistically, T3 action on UCP1 expression in sWAT depends upon cAMP and is blocked in Adipo-GsαKO mice even as elevated DNL persists. Thus, T3 enhances sWAT thermogenesis by amplifying cAMP signaling, while its control of adipocyte DNL can be mediated independently of both cAMP and rapamycin-sensitive mTORC1.

Graphical Abstract

In Brief

Guilherme et al. show that the activation of white adipose tissue thermogenesis in mice by either β3-adrenergic agonists or thyroid hormone requires both signaling pathways operating in tandem. In contrast, stimulation of *de novo* lipogenesis by these agents is dependent upon the thyroid hormone pathway.

INTRODUCTION

When exposed to cold temperatures, mammals elicit a coordinated physiological response aimed at maintaining their body temperature. This adaptive thermogenic response is initiated by the central (CNS) and sympathetic (SNS) nervous systems to elevate uncoupling protein 1 (UCP1) and heat generation in "beige" adipocytes within subcutaneous white adipose tissue (sWAT) and brown adipose tissue (BAT) (Cannon and Nedergaard, 2004; Nedergaard and Cannon, 2014). Adipose nerve fibers play a pivotal role in these processes, as disruption of adipose sympathetic innervation impairs lipolysis as well as thermogenesis and induces obesity and glucose intolerance in rodents (Bartness et al., 2014; Cannon and Nedergaard, 2004; Guilherme et al., 2019; Jiang et al., 2017; Pereira et al., 2017; Schulz et al., 2013). Cold exposure also elicits significant increases in adipocyte glucose and lipid metabolism, including glucose uptake, fatty acid oxidation, and fatty acid biosynthesis (called *de novo* lipogenesis [DNL]) (Cannon and Nedergaard, 2004; Orava et al., 2011; Yu et al., 2002). Such activation of the opposing pathways of DNL and fatty acid oxidation has been

suggested as a mechanism to ensure the availability of fatty acids as fuel to be oxidized, providing energy for heat production during thermogenesis (Mottillo et al., 2014; Yu et al., 2002). However, DNL and fatty acid oxidation in other cell types are normally regulated in a reciprocal fashion through the inhibition of the mitochondrial fatty acid uptake Cpt1 proteins by the DNL intermediate malonyl-coenzyme A (CoA), which attenuates fatty acid oxidation (Foster, 2012). In the liver, for example, this regulation ensures a predominance of the activity of one pathway over the other (Foster, 2012). The distinctive cellular signaling pathways that coordinate the simultaneous upregulation of both DNL and fatty acid oxidation within sWAT and BAT are not known.

Canonically, the sympathetic neurotransmitter norepinephrine (NE) signals through the cAMP pathway in adipocytes to upregulate lipolysis and UCP1, as well as other mitochondrial proteins that mediate fatty acid oxidation (Cannon and Nedergaard, 2004; Collins, 2012). NE activates β-adrenergic receptors (β-ARs), through which the G protein-coupled receptor Gsα stimulates adenylate cyclase and cyclic AMP (cAMP) production, activating the protein kinase A (PKA) pathway (Collins, 2012; Guilherme et al., 2019). Accordingly, sWAT sympathetic denervation (Bartness et al., 2014) or genetic deletion of adipocyte Gsα (Li et al., 2016) suppresses lipolysis and adipose thermogenesis. Furthermore, signaling by PKA through the mechanistic target of rapamycin complex 1 (mTORC1) pathway is required for optimal thermogenic responses in adipose tissue (Chen et al., 2018; Liu et al., 2016; Tran et al., 2016). Although less is known about the CNS regulation of adipocyte DNL, functional adipose sympathetic fibers also appear necessary for such regulation. Hypothalamic administration of insulin or leptin upregulates WAT DNL, and these effects are blocked by adipose sympathetic nerve fiber ablation (Buettner et al., 2008; Scherer et al., 2011). Sympathetic stimulation of DNL in BAT from cold-exposed rodents has also been previously demonstrated (Sanchez-Gurmaches et al., 2018; Trayhurn, 1979, 1980; Yu et al., 2002). Furthermore, pharmacological activation of the β3-AR in mice mimics cold exposure in activating both thermogenesis and DNL in sWAT and BAT (Lee et al., 2017; Mottillo et al., 2014). Recent data indicate that lipolysis stimulation is required for the optimal upregulation of UCP1 in sWAT (Mottillo et al., 2014), but whether the β-AR-cAMP-PKA pathway is essential for the activation of sWAT DNL during adaptive thermogenesis is less clear. These findings indicate that the SNS controls the simultaneous activation of synthesis and oxidation of fatty acids in sWAT and BAT in the cold, but the upstream signaling elements that are required for DNL regulation and how they are integrated with those that control thermogenesis are not well understood.

Based on the above considerations, the aim of the present studies was to determine how upstream β-AR signaling pathways coordinately control thermogenesis versus DNL. We focused on sWAT since the expansion of beige adipocytes expressing UCP1 within sWAT depots in humans and rodents during cold exposure indicates that they have important roles to play in systemic metabolism (Hepler et al., 2017; Ikeda et al., 2018; Langin, 2010). Recent work demonstrating the ability of beige adipocytes to secrete factors beneficial to overall glucose homeostasis has amply reinforced this concept (Kajimura et al., 2015; Min et al., 2016). In this article, we report that during cold acclimation, the signaling pathways to enhance UCP1 and DNL gene expression diverge following cAMP generation. While adrenergic upregulation of both UCP1 and DNL genes are abolished in mice deficient in

adipose tissue Gsα, rapamycin treatment to inhibit mTORC1 selectively inhibits the former. Furthermore, our findings indicate that the activation of adipose sympathetic activity stimulates local production of the thyroid hormone T3 (triiodothyronine) to induce DNL in sWAT. Thus, synthesis and oxidation of fatty acids in sWAT are simultaneously enhanced by the sustained activation of β3-AR and T3 hormone receptor (TR) signaling. However, in contrast to thermogenesis, control of adipocyte DNL by TR signaling can be mediated independently of cAMP. This cooperation between sympathetic nerve activity and thyroid hormone receptor signaling to promote both fatty acid biosynthesis and oxidation in adipose tissue may be critical to ensure lipid production as fuel for thermogenesis.

RESULTS

Expression of Genes Related to Both Fatty Acid Synthesis and Oxidation Are Coordinately Regulated by Sympathetic Nerve Activity in sWAT

Initial experiments were conducted to confirm the hypothesis that adipose SNS activity drives both thermogenesis and DNL gene expression in sWAT during cold exposure. Housing mice at 6°C for 2 weeks strongly activated the expression of lipogenic transcriptional factor ChREBPβ and the DNL genes fatty acid synthase (*Fasn*), ATP-citrate lyase (*Acly*), acetyl-CoA-carboxylase-2 (*Acacb*), and stearoyl-CoA-desaturase (*Scd1*) (Figures 1A and 1C) in concert with the expected upregulation of thermogenesis-related genes *Ucp1, Cidea*, and *Pgc1a* (Figures 1B and 1C) in sWAT. The appearance of multilocular beige adipocytes within the sWAT of these cold-exposed mice in conjunction with the appearance of UCP1 and FASN protein was also readily observed (Figure 1D). To test the requirement of sympathetic nerve activity for these effects, sWAT depots in mice were injected with vehicle (control mice) or 6-hydroxydopamine (6-OHDA) (denervated mice) in advance of 6°C cold challenge for 7 days. As shown in Figures 1E and 1F, the sympathetic nerve marker tyrosine hydroxylase (TH) was greatly reduced by the 6-OHDA treatment, indicating that denervation was extensive, while the cold-induced increased expression of genes related to both DNL and thermogenesis was virtually abolished. In addition, sympathetic denervation reduced the appearance of multi-locular adipocytes that contain FASN and UCP1 (Figure 1G). We have used mechanical denervation of sWAT as an additional approach to validate the results obtained using chemical denervation. Both chemical and mechanical denervations of sWAT greatly reduce the enhancement of DNL-related gene expressions upon cold stimulus (data not shown).

These results show that there is strong upregulation of DNL gene expression in sWAT concomitant with enhanced thermogenesis during cold exposure in mice, and that both of these responses are similarly dependent upon sympathetic signaling.

β3-AR Activation Rescues Adipose DNL at Thermoneutrality

To test whether sympathetic neurotransmitter signaling through adrenergic receptors is sufficient to stimulate DNL during 6°C cold exposure, we tested the effects of the β3-AR agonist CL316243 (CL) injected into mice. As depicted in Figures 2A and 2B, a 6-day treatment of mice at room temperature (RT) with CL stimulated the expression of several DNL-related genes in sWAT and gonadal adipose tissue (eWAT, data not shown) depots to

an extent that is similar to cold stimulus (compare to Figures 1 and 2). Among these genes are the lipogenic transcriptional factor *ChREBPβ* and the DNL enzymes *Acly, Fasn, Acacb, Scd1,* and *Elovl6*, and they are selectively upregulated in the adipocytes, but not in the stromal vascular fraction (SVF) (Figure 2C). Similar data were obtained for thermogenic gene expression (Figures 2A–2C). To test the effect of CL in the virtual absence of sympathetic signaling, mice were housed for 6 weeks at 30°C (thermoneutrality [TN]). This greatly decreased the expression of DNL genes in both BAT (Figures 2D and 2E) and sWAT (Figures 2F and 2G) and caused a "whitening" of BAT (Figure 2H). The administration of CL to mice at TN caused a sharp increase in the expression of DNL genes FASN and ACLY (Figures 2D–2G) and "browning" of both BAT and sWAT with increased multilocularity in the latter (Figures 2H and 2I). These data confirm that pharmacological stimulation of β3-AR in mice at RT or TN activates DNL in subcutaneous adipocytes, mimicking the stimulatory effect of cold exposure.

Adipocyte cAMP Signaling Is Essential for the β3-AR-Mediated Activation of DNL

Canonically, β3-AR signaling occurs via activation of Gsα-type G proteins, followed by the stimulation of adenylyl cyclase and an increased production of intracellular cAMP to regulate protein phosphorylation and gene transcription (Cannon and Nedergaard, 2004; Collins, 2012; Li et al., 2016; Reverte-Salisa et al., 2019). To establish whether cAMP signaling is required for β3-AR-mediated activation of DNL gene expression in adipocytes, we used mice with the genetic deletion of Gsα selectively in adipocytes by crossing Gsα-Flox/Flox mice with adiponectin-Cre mice to generate Adipo-GsαKO (knockout) mice, as previously described (Li et al., 2016). Gsα protein levels were reduced in adipocytes from sWAT (Figures 3A and 3B) and BAT (Figure S1), but not in adipose-derived SVFs (Figure 3B) or other tissues in Adipo-GsαKO mice, such as the liver (Figure S2), confirming the selective deletion of Gsα in adipocytes. Adipocyte lipolysis relies on β3-AR stimulation of the cAMP-PKA pathway to enhance perilipin phosphorylation and triglyceride (TAG) hydrolysis in response to CL (Li et al., 2016; Zechner et al., 2012), and accordingly, the levels of circulating free fatty acids (FFAs) were significantly reduced in Adipo-GsαKO (Figure 3C), as previously described (Li et al., 2016). While CL treatment enhanced the expression of several DNL-related genes in sWAT from control Gsα-Flox/Flox mice, the effects were not recapitulated in Adipo-GsαKO mice (Figures 3A–3E). Moreover, the β3-AR-induced expression of thermogenic genes in control mice, such as *Ucp1, Cidea, Ppargc1α, Pparγ2,* and *Pdk4*, were suppressed in the sWAT and BAT of Adipo-GsαKO mice (Figures 3A, 3F, and S1), confirming an essential role of cAMP signaling in adipose thermogenesis (Li et al., 2016; Paulo et al., 2018; Reverte-Salisa et al., 2019). Thus, cAMP signaling in adipocytes is indispensable for β3-AR-mediated activation of DNL in adipocytes, as it is for thermogenesis.

mTORC1 Is Not Essential for β3-AR-Induced Adipose DNL

Based on our previous findings that the mTORC1 is necessary for β3-AR to induce thermogenesis in sWAT (Chen et al., 2018; Liu et al., 2016; Tran et al., 2016) and about the well-known role of mTORC1 in regulating the DNL pathway in adipocytes and other cell types (Caron et al., 2015; Crewe et al., 2019; Czech et al., 2013; Danai et al., 2013; Feng et al., 2015; Han and Wang, 2018; Li et al., 2010; Peterson et al., 2011; Song et al., 2018; Youn

et al., 2019), we investigated whether mTORC1 is also required for β3-AR regulation of DNL gene expression in WAT. Mice were treated with rapamycin (2.5 mg/kg body weight per day) once per day for 2 consecutive days, before and during a 7-day 4°C cold challenge, as previously described (Liu et al., 2016). Under these experimental conditions, rapamycin treatment inhibited the cold-stimulated mTORC1 signaling pathway in adipose cells, as previously demonstrated by reductions in ribosomal S6 protein phosphorylation levels (Liu et al., 2016). However, while rapamycin-mediated mTORC1 inhibition significantly reduced the stimulatory effects of cold on the expressions of UCP1 in sWAT (Figures 4A and 4B), as previously reported (Liu et al., 2016), rapamycin treatment had no effect on cold-stimulated ACLY, FASN, and acetyl-CoA carboxylase (ACC) protein levels (Figures 4A and 4B). Furthermore, while mTORC1 inhibition via rapamycin completely blocked the CL-mediated induction of the thermogenic mediator UCP1, rapamycin failed to inhibit DNL gene expression in sWAT (Figures 4C–4E) and other adipose tissue depots under these same conditions (Figure S3). These results indicate a bifurcation in the β3-AR-cAMP signaling pathways that mediate the induction of the thermogenic gene program versus DNL in sWAT.

β3-AR Signaling Upregulates UCP1 Expression but Fails to Promote Adipose DNL *In Vitro*

The data in Figures 1, 2, 3, and 4 indicate that β3-AR activation signals through cAMP to stimulate adipocyte DNL gene transcription *in vivo*. Therefore, the question of whether β3-AR signaling activates DNL in adipocytes *in vitro* through a cell-autonomous mechanism was addressed. To this end, mature 3T3-L1 adipocytes weretreated with vehicleor with 100 nM CL for the indicated period (Figure 5A), showing that CL treatment failed to drive DNL gene expression. In fact, stimulation with CL significantly reduced the expression of several DNL-related genes in this adipocyte cell line (Figure 5A). In contrast, CL treatment strongly upregulated the expression of the thermogenic genes *Ucp1, Ppara*, and *Pgc1a* in 3T3-L1 adipocytes (Figure 5B). Consistent with these results in 3T3-L1 adipocytes, the treatment of primary adipocytes *in vitro* with CL also failed to increase the expression of DNL-related genes ACLY and FASN (Figure 5D), while PKA activation and stimulation of thermogenic gene expression were readily observed in these CL-treated primary adipocytes (Figures 5C–5E). These data are consistent with the hypothesis that although activation of PKA is sufficient to drive UCP1 expression in adipocytes, other factors or pathways are required to stimulate DNL-related gene expression.

T3 Signaling Enhances cAMP Signaling and Is Essential for β3-AR-Induced DNL in Adipocytes

We identified thyroid hormone T3 as a potential factor that may be independently required for optimal DNL regulation in sWAT based on previous data indicating that the thyroid hormone T3 can regulate lipogenesis in BAT (Bianco et al., 1998; Christoffolete et al., 2004). AR signaling has been shown to enhance BAT production of T3 through the upregulation of BAT Dio2 (iodothyronine deiodinase 2), which locally converts circulating T4 (thyroxine) to T3 (de Jesus et al., 2001; Silva and Larsen, 1983, 1985). Consistent with these studies, Dio2 expression levels were reduced in BAT and sWAT from Adipo-GsαKO mice (Figures S4B and S4C). Also, a similar increase in Dio2 in sWAT adipocytes (Figure S4A) was observed in our experiments in response to cold (Figure 6A) or CL (Figure 6B), suggesting increased local T3 concentrations. Conversely, synergism between sympathetic

signaling and thyroid hormone is known to occur through T3 potentiation of cAMP production in response to AR activation (Carvalho et al., 1996; Rubio et al., 1995a, 1995b). This concept is depicted in Figure 6K. T3 administration to wild-type mice enhanced the cAMP signaling pathway in sWAT under the conditions of our experiments, as evidenced by the potentiation of phosphorylation of downstream substrates of PKA (phospho-HSL and phospho-CREB) in response to CL administration (Figures 6F and S4B). In the same experiments, T3 treatment of mice also elevated UCP1, FASN, and ACLY protein levels. These results are consistent with a large body of work (Carvalho et al., 1996; Rubio et al., 1995a, 1995b), underscoring the feedforward cycle whereby cAMP and T3 amplify each other's activity (Figure 6K).

We next explored the dependency of AR signaling on thyroid hormone to thermogenesis (UCP1 expression), lipolysis (phospho-HSL), and DNL genes in a hypothyroid mouse model. As depicted in Figures 6D and 6E, circulating levels of T4 and T3 were strongly reduced in mice rendered hypothyroid with iodine-deficient + propylthiouracil (PTU) diet feeding. Moreover, CL treatment did not affect the plasma levels of T3 or T4 in euthyroid or hypothyroid mice, while the circulating levels of T3 were increased in both euthyroid and hypothyroid mice treated with T3, as expected.

As shown in Figure 6F, both CL and T3 treatment elicited strong upregulation of FASN and ACLY proteins in sWAT from euthyroid mice. CL administration completely failed to stimulate the expressions of FASN and ACLY in the sWAT of hypothyroid mice, showing that T3 signaling is required for β3-AR activation of DNL genes in these adipocytes. Consistent with this notion, co-administration of CL and T3 into hypothyroid mice completely rescued the β3-AR-stimulated FASN, ACLY, ChREBPβ, GLUT4, ACC2, and SCD1 expressions in sWAT (Figures 6F–6H and S4E). Similarly, β3-AR activation by CL failed to induce UCP1 expression in sWAT from hypothyroid mice (Figures 6F–6H), while coadministration of CL and T3 rescued the UCP1 upregulation in sWAT. The formation of UCP1$^+$ and FASN$^+$ multilocular adipocytes elicited by CL treatment was also completely suppressed in hypothyroid mice, while the co-administration of T3 restored the formation of such cells (Figures 6I and 6J). These results suggest that thyroid hormone T3 enhances cAMP signaling and is indispensable for optimal β3-AR stimulation of PKA, DNL, thermogenic gene expression, and browning of sWAT in subcutaneous adipocytes.

T3 Treatment Partially Restores DNL but Not Thermogenesis in Adipocytes Independently of cAMP

Having established that effective CL signaling in sWAT absolutely requires T3 function, we sought to answer the converse question: is T3 able to enhance DNL in sWAT independent of cAMP signaling? To address this issue, control and Adipo-GsαKO mice were treated with daily doses of vehicle or T3 for 10 days. As depicted in Figures 7A and 7B, T3 treatment of Gsα-Flox/Flox mice upregulated FASN and UCP1 protein expression in sWAT, which is consistent with the results observed in wild-type euthyroid mice shown in Figure 6. In contrast, the loss of cAMP production by adipocyte inactivation of Gsα completely blocked the stimulatory effect of T3 on UCP1 expression in sWAT (Figures 7A and 7B). In agreement with the UCP1 immunoblot in Figure 7A, the formation of UCP1$^+$ multilocular

adipocytes was also suppressed in sWAT from Adipo-GsαKO mice (Figure 7C). Treatment with T3 to a large extent rescued the inhibition of FASN, ACLY, ACC, and SCD1 protein expressions due to the lack of cAMP production (Figures 7A and 7B). Thus, the incremental increase in FASN, ACLY, ACC, and SCD1 protein expressions in response to T3 in Adipo-GsαKO mice was similar to what is observed in control mice (Figure 7B). While the effect of T3 treatment on UCP1 expression was minimal in adipocytes lacking cAMP, this hormone enhanced DNL gene expressions in adipocytes despite the absence of cAMP. These results suggest that while the transcriptional regulation of UCP1 by T3 requires cAMP, the activation of DNL enzymes by this hormone can occur independently of cAMP signaling. Therefore, these results are consistent with a working model whereby β3-AR-mediated local T3 production stimulates the transcriptional activity of TRs to promote the expression of DNL-related genes and potentiates the cAMP-PKA pathway that is essential for thermogenic gene expression in adipocytes (Figure 7D).

To further investigate whether the lack of proper CL and T3 responses observed in the constitutive Adipo-GsαKO mice were due to developmental issues that arise from the absence of cAMP in adipocytes at an early life stage, we generated a tamoxifen-inducible KO mouse model of Gsα deficiency called inducible Adipo-GsαKO (iAdipo-GsαKO). We then conducted experiments wherein Gsα protein deletion was induced in adipocytes by treating mature adult iAdipo-GsαKO mice with tamoxifen, as depicted in Figure S6A. Two weeks post-tamoxifen injections, mice were then treated or not treated with CL316243 or with T3 and the effect of these agonists on UCP1 expression in sWAT evaluated. As shown in Figure S6, tamoxifen treatment inhibited the Gsα expression levels in sWAT from iAdipo-GsαKO, but not Gsα-Flox/Flox mice. Both CL316243 and T3 failed to induce UCP1 expression in sWAT from iAdipo-GsαKO, suggesting that early developmental defects that may hypothetically arise from early cAMP deficiency do not account for the inhibition of the T3 response (Figures 3, 7, and S6). Moreover, these findings further reinforce the essential role played by cAMP during T3/TR signaling to promote UCP1 expression in white adipocytes.

Also, if permanent developmental disruptions occurred in the constitutive Adipo-GsαKO mice that disrupted cell responsiveness, then such adipocytes from these mice should not respond to acute stimulation by cAMP itself (e.g., an acute rescue). To address this question, adipose tissue explants excised from the Adipo-GsαKO mice were acutely incubated with dibutyryl cAMP *in vitro* to test whether they would regain responsiveness. As shown in Figure S5, adipose tissue depleted of Gsα protein treated with dibutyryl-cAMP, but not with β3-agonist CL, regained responsiveness, as both PKA activity and lipolysis were stimulated by dibutyryl cAMP treatment. Moreover, UCP1 expression in subcutaneous adipocytes lacking Gsα was strongly stimulated by dibutyryl-cAMP treatment, but not by CL. These results suggest that nonspecific cellular deficiencies due to the absence of cAMP in adipocytes during development is not the cause of blockade in T3 actions on thermogenesis in sWAT.

DISCUSSION

The main findings presented here demonstrate an obligatory link between signaling by sympathetic nerve fibers in adipose tissue via the β3-AR-cAMP-PKA pathway and T3/TR signaling to promote both thermogenesis and DNL in sWAT during cold exposure. β3-AR agonist administration cannot stimulate either UCP1 expression or DNL gene expression in sWAT in the absence of thyroid hormone, while T3 administration rescues these responses (Figure 6). Our results reveal that the relationship between the cAMP pathway and T3 signaling differs mechanistically for UCP1 versus DNL gene regulation. In the case of UCP1 expression, the major role of T3 is to amplify cAMP signaling (Figure 6F), likely by increasing the generation of cAMP itself. Thus, T3 administration has little effect on its own to enhance UCP1 expression in the absence of cAMP signaling, as observed in Adipo-GsαKO mice (Figures 7A–7C and S6) or following induction of the Gsα in mature iAdipo-GsαKO mice (Figure S6). In contrast, β3-AR-cAMP-PKA signaling to elevate DNL gene expression appears to be driven to a large extent through the DIO2-mediated conversion of T4 to T3 (Figure 6A), which can elevate FASN and other DNL enzymes independent of cAMP (Figure 7).

It is noted that previous work by several laboratories (Finan et al., 2016; Johann et al., 2019; Lin et al., 2015; Matesanz et al., 2017) has shown that T3 and TR agonists stimulate sWAT thermogenesis in the absence of β3-AR agonists, and that this can occur even when mice are housed at TN (Johann et al., 2019; Lin et al., 2015). This work has suggested the idea that T3 may act on UCP1 expression independent of the cAMP pathway. However, none of these studies tested the effects of TR agonists in mice deficient in the ability to produce cAMP, as we present here. Thus, our data make the important point that T3 actions on sWAT thermogenesis cannot occur in the total absence of cAMP and that further work is necessary to fully understand the molecular basis for this relationship between cAMP and T3 actions in sWAT.

Increased local production of T3 in BAT via the sympathetic activation of DIO2 has been described in previous reports (de Jesus et al., 2001; Silva and Larsen, 1983, 1985). Genetic deletion of DIO2 completely abolishes the activation of DNL in brown adipocytes from mice exposed to 4°C (Christoffolete et al., 2004). Consistent with a significant role of TRs in the regulation of adipocyte fatty acid biosynthesis, several DNL-related genes, such as ChREBP, Fasn, Acaca, Me, Thrsp, and Slc2a4, present TR-binding sites in their promoter regions (thyroid-responsive elements [TREs]), and their expressions in BAT and in white adipocytes are upregulated by thyroid hormone treatment both *in vivo* and *in vitro* (Bianco et al., 1998; Blennemann et al., 1995; Katz et al., 2018; Moustaid and Sul, 1991; Obregon, 2014). Moreover, conversion of ^{14}C-glucose into TAGs and fatty acids are enhanced in sWAT from mice treated with T3 and β3-AR agonist CL (Figure S4). Thus, the increases in the expression of DNL genes in response to T3 and CL are accompanied by the expected increase in metabolic flux through the DNL pathway. These results suggest that adipose sympathetic drive relies on both β3-AR and TR signaling in an integrated mode to optimally activate adipocyte DNL gene expression and DNL metabolic flux during adaptive thermogenesis (Figure 7D).

The concept that a bifurcation in cAMP signaling related to UCP1 versus DNL gene expression occurs at relatively early steps in the pathway is also consistent with our findings on the role of mTORC1 in these processes. Previous work by us (Liu et al., 2016) and others (Chen et al., 2018; Tran et al., 2016) has demonstrated that mTORC1 (mTOR and Raptor) operates downstream of β3-AR and is essential for adipose thermogenesis and browning induced by β3-AR activation. Based on the results of many studies indicating a regulatory role of mTORC1 to control DNL in the liver (Caron et al., 2015; Feng et al., 2015; Han and Wang, 2018; Li et al., 2010; Peterson et al., 2011; Youn et al., 2019) and adipose tissue (Crewe et al., 2019; Czech et al., 2013; Danai et al., 2013; Song et al., 2018), it seemed likely that mTORC1 may also mediate the stimulatory effect of β3-AR on adipocyte DNL. This does not seem to be the case, as rapamycin treatment of mice completely blocked cold-induced UCP1 expression in sWAT but failed to blunt the activation of adipose DNL by cold exposure (Figure 4). Therefore, rapamycin-sensitive mTORC1 activities that mediate the effects of β3-AR activation on adaptive adipose thermogenesis are not essential for β3-AR to activate sWAT DNL at cold temperatures. These findings are consistent with the concept that T3 primarily enhances the early steps of cAMP signaling (Figure 7D).

While the present studies were directed to early events that control DNL gene expression in response to SNS activation, clearly, the mechanisms at play at the transcriptional level are also crucial to a full understanding of DNL regulation. It is of interest that DNL gene regulation is also under the control of insulin signaling (Czech, 2017; Czech et al., 2013; Guilherme et al., 2017), suggesting that there may be additional coordinated integration of T3 action with the downstream effects of insulin. Additional research on how transcriptional regulators are coordinately controlled by inputs from cAMP, insulin, and T3 to control DNL genes will be of great interest to the field.

STAR★METHODS

RESOURCE AVAILABILITY

Lead Contact—Further information and requests for resources and reagents should be directed to and will be fulfilled by the Lead Contact Dr. Michael P Czech (Michael.Czech@umassmed.edu).

Material Availability—This study did not generate new unique reagents.

Data and Code Availability—This study did not generate any unique datasets or code.

EXPERIMENTAL MODEL AND SUBJECT DETAILS

Mice were housed on a 12 h light/dark schedule, and except when indicated, had free access to water and food. All of the studies performed were approved by the Institutional Animal Care and Use Committee (IACUC) of the University of Massachusetts Medical School. Mice with conditional Gsα–Flox/Flox alleles were generated as previously described (Li et al., 2016). Mice were analyzed between 6-16 weeks of age. Both male and female mice were used for analysis. To selectively delete Gsα (*Gnas*) in adipocytes from mice, homozygous Gsα–Flox/Flox animals were crossed to Adiponectin-Cre mice (B6;FVB-Tg(Adipoq-

cre)1Evdr/J) to generate the adipocyte-specific knockout mice referred to as Adipo-GsαKO. To inactivate Gsα in adipocytes from adult mice, Gsα-Flox/Flox mice were crossed to Adiponectin-Cre-ERT2 mice (B6.129-Tg(Adipoq-cre/Esr1*)1Evdr/J) to generate an tamoxifen-inducible iAdipo-GsαKO mouse line. The induction of Gsα deletion in adipocytes of 6 week-old mature iAdipo-GsαKO female mice were then carried out via intraperitoneal injections (i.p.) of tamoxifen, as previously described (Guilherme et al., 2017). For CL316243 treatment of the GsαKO mice, at the indicated weeks of age (Figure S6), both control Gsα–Flox/Flox and Adipo-GsαKO were treated via i.p. injection once a day with saline vehicle or with 5 mg/kg CL316243 for 6 consecutive days. On the next day, adipose tissue was harvested and processed for histological and biochemical analyses. Serum nonesterified fatty acid (NEFA) levels were measured using a colorimetric assay (Fujifilm Wako Diagnostics) according to the manufacturer's instructions.

METHOD DETAILS

Adipose Tissue Denervation—To examine the contribution of adipose sympathetic activity to cold-induced DNL in adipocytes, sympathetic nerve fibers in subcutaneous inguinal fat from 12 week-old C57BL/6J male mice were chemically destroyed with 6-hydroxydopamine (6-OHDA) by direct injection into adipose depots as previously described (Vaughan et al., 2014). Ten days post-injection, mice were placed at 6°C for 7 days and adipose tissue depots were then harvested and reductions in tyrosine hydroxylase content in sWAT examined to confirm efficient denervation. For surgical denervation of subcutaneous inguinal fat nerves, denervation surgery was performed on sWAT from C57BL/6 as previously reported (Vaughan et al., 2014). Briefly, mice were anesthetized with isoflurane and then a ventral lateral incision was made to expose sWAT nerves innervating the sWAT were either left intact (Sham control) or surgically destroyed as described (Vaughan et al., 2014)

Animal Housing at Thermoneutral Temperature and β3-AR-agonist Treatment —For the effects of thermoneutrality on adipose tissue DNL gene expression, 8-week-old C57BL6/J male mice were kept either at 22°C (mild-cold) or transferred from mild-cold to 30° C (thermoneutrality) and acclimated for 6 weeks. Then, mice were treated with 5 mg/kg of β3-agonist CL316243 or phosphate-buffered saline (PBS) (one daily i.p. injection for 6 days). One day following the final injection, adipose tissue was harvested and processed for histological and biochemical analyses.

Rapamycin Treatment—To evaluate the effects of rapamycin on cold- and CL316243-stimulated adipose DNL, mice were treated with rapamycin as previously described (Liu et al., 2016). Briefly, 12-14 week-old C57BL/6J male mice were administered with vehicle (75% saline, 10% ethanol, 10% PEG 300, 5% Tween 80) or rapamycin (2.5 mg/kg body weight/day) once a day for 2 consecutive days. On the third day, the mice were housed individually and placed at 4°C for 7 days with daily rapamycin administration. Control mice were maintained at room temperature (22°C). For selective activation of β3-AR, mice were treated with rapamycin (2.5 mg/kg body weight/day) for 2 days and then treated with vehicle or with CL316243 (5 mg/kg/day) with daily rapamycin administration for 7 days. Adipose

tissue depots (sWAT, eWAT and BAT) were then harvested and processed for histological and biochemical analyses.

Hypothyroid Mouse Model and T3 Treatment—Mice were rendered hypothyroid induced by feeding 8 week-old C57BL6/J male mice an iodine-deficient chow diet supplemented with 0.15% propylthiouracil (PTU, catalog TD.95125; ENVIGO) for 7 weeks. Euthyroid mice fed chow diet (ingredient matched, plus iodine and without PTU, catalog TD.97350; ENVIGO) served as controls. This protocol has been shown to lead to a hypothyroid state in mice fed an iodine-deficient plus PTU diet, as determined by circulating thyroxine (T4) and triiodothyronine (T3) measurements. Serum levels of T4 and T3 were measured by ELISA (Calbiotech) after 7 weeks of treatment. Two additional groups of mice were rendered hypothyroid as above and after 6 weeks of treatment one group were treated with CL316243 (5 mg/kg body weight) and the other group co-treated with CL316243 (5 mg/kg body weight) plus T3 (25mg/kg of body weight) via i.p. injections during 10 days, while remaining in iodine-deficient diet plus PTU.

Lipogenesis Assay—To assess lipogenesis in white adipose tissue, sWAT explants were incubated with labeling media containing 0.2% fatty acid-free BSA, 0.5 mM D(+)-Glucose, 0.5 mM sodium acetate, 2 mM sodium pyruvate, 2 mM L-glutamine, and 2 μCi/mL [^{14}C]-U-glucose as described (Danai et al., 2013; Guilherme et al., 2017; Pedersen et al., 2015). Adipose tissue explants were incubated at 37°C in a humidified incubator (5% CO2) for 4.5 h before total neutral lipid extraction. Glucose incorporation into triglyceride-fatty acids (TG-Fatty acids) or into triglyceride-glycerol (TG-Glyceride) was then determined as previously described (Danai et al., 2013; Guilherme et al., 2017; Pedersen et al., 2015; Rodbell, 1964).

Adipocyte Cell Cultures—For experiments with 3T3-L1 mature adipocytes, 3T3-L1 fibroblasts were obtained from ATCC, maintained and differentiated into adipocytes as previously described (Pedersen et al., 2015). On the seventh day after differentiation, mature adipocytes were treated with CL316243 as stated in figure legend for the indicated period of time. Cells were then harvested and total RNA extracted and used for quantitative RT-PCR analysis. For the experiment with primary adipocytes, primary subcutaneous white fat stromal vascular fraction (SVF) from 3 weeks of age C57BL6/J mice was isolated according to published methods (Danai et al., 2015; Guilherme et al., 2017). Briefly, primary SVF cells were cultured in DMEM/F12 containing 10% Fetal Bovine Serum (FBS), 100 U mL^{-1} penicillin, 0.1 mg mL^{-1} streptomycin and 0.1 mg mL^{-1} normocin (maintenance medium) until full confluence. Then, adipocyte differentiation was induced in preadipocyte cultures as previously described (Guilherme et al., 2017). To examine the effects of β3-AR activation on DNL gene expression in mature primary adipocytes, at day 7th-post differentiation adipocytes were incubated with the indicated CL316243 concentrations for 6h on the seventh day post-differentiation, followed by total protein or RNA extractions for immunoblotting or qPCR quantification.

Dibutyryl-cAMP Treatment—To evaluate the effects of acute treatment of dibutyryl-cAMP in sWAT adipocytes, subcutaneous preadipocytes in the SVF cells from 3 weeks of

age Gsα-Flox/Flox and Adipo-GsαKO mice were cultured in maintenance medium until full confluence. Cells were then differentiated into adipocyte and at the 7th days-post differentiation, control and GsαKO mature adipocytes were incubated with vehicle, CL316243 0.2 mM or dibutyryl-cAMP 1 mM and their effects on lipolysis, and UCP1 expression levels examined. Media from these cells were also collected after 2.5h of incubation and the levels of glycerol released in the media determined using colorimetric assay to measure free glycerol. To assess the effects of dibutyryl-cAMP treatment on adipose tissue deleted of Gsα, sWAT explants from Gsα-Flox/Flox and Adipo-GsαKO mice were incubated at 37°C with media containing CL316243 0.2 mM or dibutyryl-cAMP for 2.5 h and the effect of these agonist on phospho-PKA substrate protein levels and on lipolysis determined by anti-PKAS immunoblot and colorimetric assay to measure free glycerol levels.

Western Blot Analysis—Cultured adipocytes or adipose tissue were lysed. Total lysates were resolved by SDS-PAGE and electrotransferred to nitrocellulose membranes. Membranes were incubated with the indicated antibodies overnight at 4°C. Immunoblots were washed with TBS-T (0.2% Tween 20 in Tris-buffered saline), incubated with horseradish peroxidase (HRP) anti-mouse or anti-rabbit secondary antibody and visualized using an enhanced chemiluminescent substrate kit (Perkin Elmer) and images taken using theChemiDoc Imaging System XRS+ with Image Lab 5.0 software. Densitometric analyses of the protein bands were performed using ImageJ Software.

RNA Isolation and RT-qPCR—Total RNA was isolated from mouse tissue using QIAzol Lysis Reagent (QIAGEN) following the manufacturer's instructions. cDNA was synthesized from isolated RNA using iScript cDNA Synthesis Kit (BioRad). Quantitative RT-PCR was performed using iQ Sybr-Green supermix (BioRad) on a BioRad CFX97 RT-PCR system and analyzed as previously described (Livak and Schmittgen, 2001; Schmittgen and Livak, 2008). *36B4, Hprt, Gapdh, 18S* and *B2m* served as controls for normalization. Primer sequences used for qRT-PCR analyses are listed in Table S1.

Histological Analysis—For immunohistochemistry (IHC), tissue samples were fixed in 4% paraformaldehyde and embedded in paraffin. Sectioned slides were then stained for FASN (Abcam) and UCP1 (Abcam) at the UMASS Medical School Morphology Core. Photos of stained sections were taken with a Leica DM2500 LED optical microscope equipped with a Leica MC170 HD camera.

QUANTIFICATION AND STATISTICAL ANALYSIS

Data were analyzed in GraphPad Prism 8 (GraphPad Software, Inc.). Student's *t*-test or the Mann-Whitney *U*-test was employed for the parametric and non-parametric data, respectively. Comparisons between more than 2 groups were performed using ANOVAwith Tukey's post hoc test. The significance level was set at p   0.05. Information on replicates/ error bars is included in the figure legends.

Supplementary Material

Refer to Web version on PubMed Central for supplementary material.

ACKNOWLEDGMENTS

REFERENCES

Bartness TJ, Liu Y, Shrestha YB, and Ryu V (2014). Neural innervation of white adipose tissue and the control of lipolysis. Front. Neuroendocrinol. 35, 473–493. [PubMed: 24736043]

Bianco AC, Carvalho SD, Carvalho CR, Rabelo R, and Moriscot AS (1998). Thyroxine 5′-deiodination mediates norepinephrine-induced lipogenesis in dispersed brown adipocytes. Endocrinology 139, 571–578. [PubMed: 9449627]

Blennemann B, Leahy P, Kim TS, and Freake HC (1995). Tissue-specific regulation of lipogenic mRNAs by thyroid hormone. Mol. Cell. Endocrinol. 110, 1–8. [PubMed: 7672439]

Buettner C, Muse ED, Cheng A, Chen L, Scherer T, Pocai A, Su K, Cheng B, Li X, Harvey-White J, et al. (2008). Leptin controls adipose tissue lipogenesis via central, STAT3-independent mechanisms. Nat. Med. 14, 667–675. [PubMed: 18516053]

Cannon B, and Nedergaard J (2004). Brown adipose tissue: function and physiological significance. Physiol. Rev. 84, 277–359. [PubMed: 14715917]

Caron A, Richard D, and Laplante M (2015). The Roles of mTOR Complexes in Lipid Metabolism. Annu. Rev. Nutr. 35, 321–348. [PubMed: 26185979]

Carvalho SD, Bianco AC, and Silva JE (1996). Effects of hypothyroidism on brown adipose tissue adenylyl cyclase activity. Endocrinology 137, 5519–5529. [PubMed: 8940379]

Chen S, Mei X, Yin A, Yin H, Cui XB, and Chen SY (2018). Response gene to complement 32 suppresses adipose tissue thermogenic genes through inhibiting β3-adrenergic receptor/mTORC1 signaling. FASEB J. 32, 4836–4847. [PubMed: 29579398]

Christoffolete MA, Linardi CC, de Jesus L, Ebina KN, Carvalho SD, Ribeiro MO, Rabelo R, Curcio C, Martins L, Kimura ET, and Bianco AC (2004). Mice with targeted disruption of the Dio2 gene have cold-induced over-expression of the uncoupling protein 1 gene butfail to increase brown adipose tissue lipogenesis and adaptive thermogenesis. Diabetes 53, 577–584. [PubMed: 14988240]

Collins S (2012). -Adrenoceptor Signaling Networks in Adipocytes for Recruiting Stored Fat and Energy Expenditure. Front. Endocrinol. (Lausanne) 2, 102. [PubMed: 22654837]

Crewe C, Zhu Y, Paschoal VA, Joffin N, Ghaben AL, Gordillo R, Oh DY, Liang G, Horton JD, and Scherer PE (2019). SREBP-regulated adipocyte lipogenesis is dependent on substrate availability and redox modulation of mTORC1. JCI Insight 5, 129397. [PubMed: 31310592]

Czech MP (2017). Insulin action and resistance in obesity and type 2 diabetes. Nat. Med. 23, 804–814. [PubMed: 28697184]

Czech MP, Tencerova M, Pedersen DJ, and Aouadi M (2013). Insulin signalling mechanisms for triacylglycerol storage. Diabetologia 56, 949–964. [PubMed: 23443243]

Danai LV, Guilherme A, Guntur KV, Straubhaar J, Nicoloro SM, and Czech MP (2013). Map4k4 suppresses Srebp-1 and adipocyte lipogenesis independent of JNK signaling. J. Lipid Res. 54, 2697–2707. [PubMed: 23924694]

Danai LV, Flach RJ, Virbasius JV, Menendez LG, Jung DY, Kim JH, Kim JK, and Czech MP (2015). Inducible Deletion of Protein Kinase Map4k4 in Obese Mice Improves Insulin Sensitivity in Liver and Adipose Tissues. Mol. Cell. Biol. 35, 2356–2365. [PubMed: 25918248]

de Jesus LA, Carvalho SD, Ribeiro MO, Schneider M, Kim SW, Harney JW, Larsen PR, and Bianco AC (2001). The type 2 iodothyronine deiodinase is essential for adaptive thermogenesis in brown adipose tissue. J. Clin. Invest. 108, 1379–1385. [PubMed: 11696583]

Feng D, Youn DY, Zhao X, Gao Y, Quinn WJ 3rd, Xiaoli AM, Sun Y, Birnbaum MJ, Pessin JE, and Yang F (2015). mTORC1 Down-Regulates Cyclin-Dependent Kinase 8 (CDK8) and Cyclin C (CycC). PLoS One 10, e0126240. [PubMed: 26042770]

Finan B, Clemmensen C, Zhu Z, Stemmer K, Gauthier K, Muller L, De Angelis M, Moreth K, Neff F, Perez-Tilve D, et al. (2016). Chemical Hybridization of Glucagon and Thyroid Hormone Optimizes Therapeutic Impact for Metabolic Disease. Cell 167, 843–857.e14. [PubMed: 27720451]

Foster DW (2012). Malonyl-CoA: the regulator of fatty acid synthesis and oxidation. J. Clin. Invest. 122, 1958–1959. [PubMed: 22833869]

Guilherme A, Pedersen DJ, Henchey E, Henriques FS, Danai LV, Shen Y, Yenilmez B, Jung D, Kim JK, Lodhi IJ, et al. (2017). Adipocyte lipid synthesis coupled to neuronal control of thermogenic programming. Mol. Metab. 6, 781–796. [PubMed: 28752043]

Guilherme A, Henriques F, Bedard AH, and Czech MP (2019). Molecular pathways linking adipose innervation to insulin action in obesity and diabetes mellitus. Nat. Rev. Endocrinol. 15, 207–225. [PubMed: 30733616]

Han J, and Wang Y (2018). mTORC1 signaling in hepatic lipid metabolism. Protein Cell 9, 145–151. [PubMed: 28434145]

Hepler C, Shao M, Xia JY, Ghaben AL, Pearson MJ, Vishvanath L, Sharma AX, Morley TS, Holland WL, and Gupta RK (2017). Directing visceral white adipocyte precursors to a thermogenic adipocyte fate improves insulin sensitivity in obese mice. eLife 6, e27669. [PubMed: 28722653]

Ikeda K, Maretich P, and Kajimura S (2018). The Common and Distinct Features of Brown and Beige Adipocytes. Trends Endocrinol. Metab. 29, 191–200. [PubMed: 29366777]

Jiang H, Ding X, Cao Y, Wang H, and Zeng W (2017). Dense Intra-adipose Sympathetic Arborizations Are Essential for Cold-Induced Beiging of Mouse White Adipose Tissue. Cell Metab. 26, 686–692.e3. [PubMed: 28918935]

Johann K, Cremer AL, Fischer AW, Heine M, Pensado ER, Resch J, Nock S, Virtue S, Harder L, Oelkrug R, et al. (2019). Thyroid-Hormone-Induced Browning of White Adipose Tissue Does Not Contribute to Thermogenesis and Glucose Consumption. Cell Rep. 27, 3385–3400.e3. [PubMed: 31189119]

Kajimura S, Spiegelman BM, and Seale P (2015). Brown and Beige Fat: Physiological Roles beyond Heat Generation. Cell Metab. 22, 546–559. [PubMed: 26445512]

Katz LS, Xu S, Ge K, Scott DK, and Gershengorn MC (2018). T3 and Glucose Coordinately Stimulate ChREBP-Mediated Ucp1 Expression in Brown Adipocytes From Male Mice. Endocrinology 159, 557–569. [PubMed: 29077876]

Langin D (2010). Recruitment of brown fat and conversion of white into brown adipocytes: strategies to fight the metabolic complications of obesity? Biochim. Biophys. Acta 1801, 372–376. [PubMed: 19782764]

Lee YH, Kim SN, Kwon HJ, and Granneman JG (2017). Metabolic heterogeneity of activated beige/brite adipocytes in inguinal adipose tissue. Sci. Rep. 7, 39794. [PubMed: 28045125]

Li S, Brown MS, and Goldstein JL (2010). Bifurcation of insulin signaling pathway in rat liver: mTORC1 required for stimulation of lipogenesis, but not inhibition of gluconeogenesis. Proc. Natl. Acad. Sci. USA 107, 3441–3446. [PubMed: 20133650]

Li YQ, Shrestha YB, Chen M, Chanturiya T, Gavrilova O, and Weinstein LS (2016). Gsα deficiency in adipose tissue improves glucose metabolism and insulin sensitivity without an effect on body weight. Proc. Natl. Acad. Sci. USA 113, 446–451. [PubMed: 26712027]

Lin JZ, Martagón AJ, Cimini SL, Gonzalez DD, Tinkey DW, Biter A, Baxter JD, Webb P, Gustafsson JA, Hartig SM, and Phillips KJ (2015). Pharmacological Activation of Thyroid Hormone Receptors Elicits a Functional Conversion of White to Brown Fat. Cell Rep. 13, 1528–1537. [PubMed: 26586443]

Liu D, Bordicchia M, Zhang C, Fang H, Wei W, Li JL, Guilherme A, Guntur K, Czech MP, and Collins S (2016). Activation of mTORC1 is essential for β-adrenergic stimulation of adipose browning. J. Clin. Invest. 126, 1704–1716. [PubMed: 27018708]

Livak KJ, and Schmittgen TD (2001). Analysis of relative gene expression data using real-time quantitative PCR and the 2(-Delta Delta C(T)) Method. Methods 25, 402–408. [PubMed: 11846609]

Matesanz N, Bernardo E, Acín-Pérez R, Manieri E, Pérez-Sieira S, Hernández-Cosido L, Montalvo-Romeral V, Mora A, Rodríguez E, Leiva-Vega L, et al. (2017). MKK6 controls T3-mediated browning of white adipose tissue. Nat. Commun. 8, 856. [PubMed: 29021624]

Min SY, Kady J, Nam M, Rojas-Rodriguez R, Berkenwald A, Kim JH, Noh HL, Kim JK, Cooper MP, Fitzgibbons T, et al. (2016). Human 'brite/beige' adipocytes develop from capillary networks, and their implantation improves metabolic homeostasis in mice. Nat. Med. 22, 312–318. [PubMed: 26808348]

Mottillo EP, Balasubramanian P, Lee YH, Weng C, Kershaw EE, and Granneman JG (2014). Coupling of lipolysis and de novo lipogenesis in brown, beige, and white adipose tissues during chronic β3-adrenergic receptor activation. J. Lipid Res. 55, 2276–2286. [PubMed: 25193997]

Moustaïd N, and Sul HS (1991). Regulation of expression of the fatty acid synthase gene in 3T3-L1 cells by differentiation and triiodothyronine. J. Biol. Chem. 266, 18550–18554. [PubMed: 1917977]

Nedergaard J, and Cannon B (2014). The browning of white adipose tissue: some burning issues. Cell Metab. 20, 396–407. [PubMed: 25127354]

Obregon MJ (2014). Adipose tissues and thyroid hormones. Front. Physiol. 5, 479. [PubMed: 25566082]

Orava J, Nuutila P, Lidell ME, Oikonen V, Noponen T, Viljanen T, Scheinin M, Taittonen M, Niemi T, Enerbäck S, and Virtanen KA (2011). Different metabolic responses of human brown adipose tissue to activation by cold and insulin. Cell Metab. 14, 272–279. [PubMed: 21803297]

Paulo E, Wu D, Wang Y, Zhang Y, Wu Y, Swaney DL, Soucheray M, Jimenez-Morales D, Chawla A, Krogan NJ, and Wang B (2018). Sympathetic inputs regulate adaptive thermogenesis in brown adipose tissue through cAMP-Salt inducible kinase axis. Sci. Rep. 8, 11001. [PubMed: 30030465]

Pedersen DJ, Guilherme A, Danai LV, Heyda L, Matevossian A, Cohen J, Nicoloro SM, Straubhaar J, Noh HL, Jung D, et al. (2015).A major role of insulin in promoting obesity-associated adipose tissue inflammation. Mol. Metab. 4, 507–518. [PubMed: 26137438]

Pereira MM, Mahú I, Seixas E, Martinéz-Sánchez N, Kubasova N, Pirzgalska RM, Cohen P, Dietrich MO, López M, Bernardes GJ, and Domingos AI (2017). A brain-sparing diphtheria toxin for chemical genetic ablation of peripheral cell lineages. Nat. Commun. 8, 14967. [PubMed: 28367972]

Peterson TR, Sengupta SS, Harris TE, Carmack AE, Kang SA, Balderas E, Guertin DA, Madden KL, Carpenter AE, Finck BN, and Sabatini DM (2011). mTOR complex 1 regulates lipin 1 localization to control the SREBP pathway. Cell 146, 408–420. [PubMed: 21816276]

Reverte-Salisa L, Sanyal A, and Pfeifer A (2019). Role of cAMP and cGMP Signaling in Brown Fat. Handb. Exp. Pharmacol. 251, 161–182. [PubMed: 29633180]

Rodbell M (1964). Metabolism of Isolated Fat Cells. I. Effects of Hormones on Glucose Metabolism and Lipolysis. J. Biol. Chem. 239, 375–380. [PubMed: 14169133]

Rubio A, Raasmaja A, Maia AL, Kim KR, and Silva JE (1995a). Effects of thyroid hormone on norepinephrine signaling in brown adipose tissue. I. Beta 1- and beta 2-adrenergic receptors and cyclic adenosine 3',5'-monophosphate generation. Endocrinology 136, 3267–3276. [PubMed: 7628360]

Rubio A, Raasmaja A, and Silva JE (1995b). Thyroid hormone and norepinephrine signaling in brown adipose tissue. II: Differential effects of thyroid hormone on beta 3-adrenergic receptors in brown and white adipose tissue. Endocrinology 136, 3277–3284. [PubMed: 7628361]

Sanchez-Gurmaches J, Tang Y, Jespersen NZ, Wallace M, Martinez Calejman C, Gujja S, Li H, Edwards YJK, Wolfrum C, Metallo CM, et al. (2018). Brown Fat AKT2 Is a Cold-Induced Kinase that Stimulates ChREBP-Mediated De Novo Lipogenesis to Optimize Fuel Storage and Thermogenesis. Cell Metab. 27, 195–209.e6. [PubMed: 29153407]

Scherer T, O'Hare J, Diggs-Andrews K, Schweiger M, Cheng B, Lindtner C, Zielinski E, Vempati P, Su K, Dighe S, et al. (2011). Brain insulin controls adipose tissue lipolysis and lipogenesis. Cell Metab. 13, 183–194. [PubMed: 21284985]

Schmittgen TD, and Livak KJ (2008). Analyzing real-time PCR data by the comparative C(T) method. Nat. Protoc. 3, 1101–1108. [PubMed: 18546601]

Schulz TJ, Huang P, Huang TL, Xue R, McDougall LE, Townsend KL, Cypess AM, Mishina Y, Gussoni E, and Tseng YH (2013). Brown-fat paucity due to impaired BMP signalling induces compensatory browning of white fat. Nature 495, 379–383. [PubMed: 23485971]

Silva JE, and Larsen PR (1983). Adrenergic activation of triiodothyronine production in brown adipose tissue. Nature 305, 712–713. [PubMed: 6633638]

Silva JE, and Larsen PR (1985). Potential of brown adipose tissue type II thyroxine 5′-deiodinase as a local and systemic source of triiodothyronine in rats. J. Clin. Invest. 76, 2296–2305. [PubMed: 4077981]

Song Z, Xiaoli AM, and Yang F (2018). Regulation and Metabolic Significance of De Novo Lipogenesis in Adipose Tissues. Nutrients 10, E1383. [PubMed: 30274245]

Tran CM, Mukherjee S, Ye L, Frederick DW, Kissig M, Davis JG, Lamming DW, Seale P, and Baur JA (2016). Rapamycin Blocks Induction of the Thermogenic Program in White Adipose Tissue. Diabetes 65, 927–941. [PubMed: 26858361]

Trayhurn P (1979). Fatty acid synthesis in vivo in brown adipose tissue, liver and white adipose tissue of the cold-acclimated rat. FEBS Lett. 104, 13–16. [PubMed: 477972]

Trayhurn P (1980). Fatty acid synthesis in brown adipose tissue in relation to whole body synthesis in the cold-acclimated golden hamster (Mesocricetus auratus). Biochim. Biophys. Acta 620, 10–17. [PubMed: 7417474]

Vaughan CH, Zarebidaki E, Ehlen JC, and Bartness TJ (2014). Analysis and measurement of the sympathetic and sensory innervation of white and brown adipose tissue. Methods Enzymol. 537, 199–225. [PubMed: 24480348]

Youn DY, Xiaoli AM, Kwon H, Yang F, and Pessin JE (2019). The subunit assembly state ofthe Mediator complex is nutrient-regulated and is dysregulated in a genetic model of insulin resistance and obesity. J. Biol. Chem. 294,9076–9083. [PubMed: 31028171]

Yu XX, Lewin DA, Forrest W, and Adams SH (2002). Cold elicits the simultaneous induction of fatty acid synthesis and beta-oxidation in murine brown adiposetissue: prediction from differential gene expression and confirmation in vivo. FASEB J. 16, 155–168. [PubMed: 11818363]

Zechner R, Zimmermann R, Eichmann TO, Kohlwein SD, Haemmerle G, Lass A, and Madeo F (2012). FAT SIGNALS-lipases and lipolysis in lipid metabolism and signaling. Cell Metab. 15, 279–291. [PubMed: 22405066]

Highlights

- TR or β3-AR can stimulate both DNL and thermogenesis (UCP1) in white adipocytes

- The induction of adipocyte DNL and UCP1 by the β3-AR is blocked in hypothyroid mice

- Conversely, TR regulates DNL but not UCP1 in adipocytes lacking β3-AR signaling

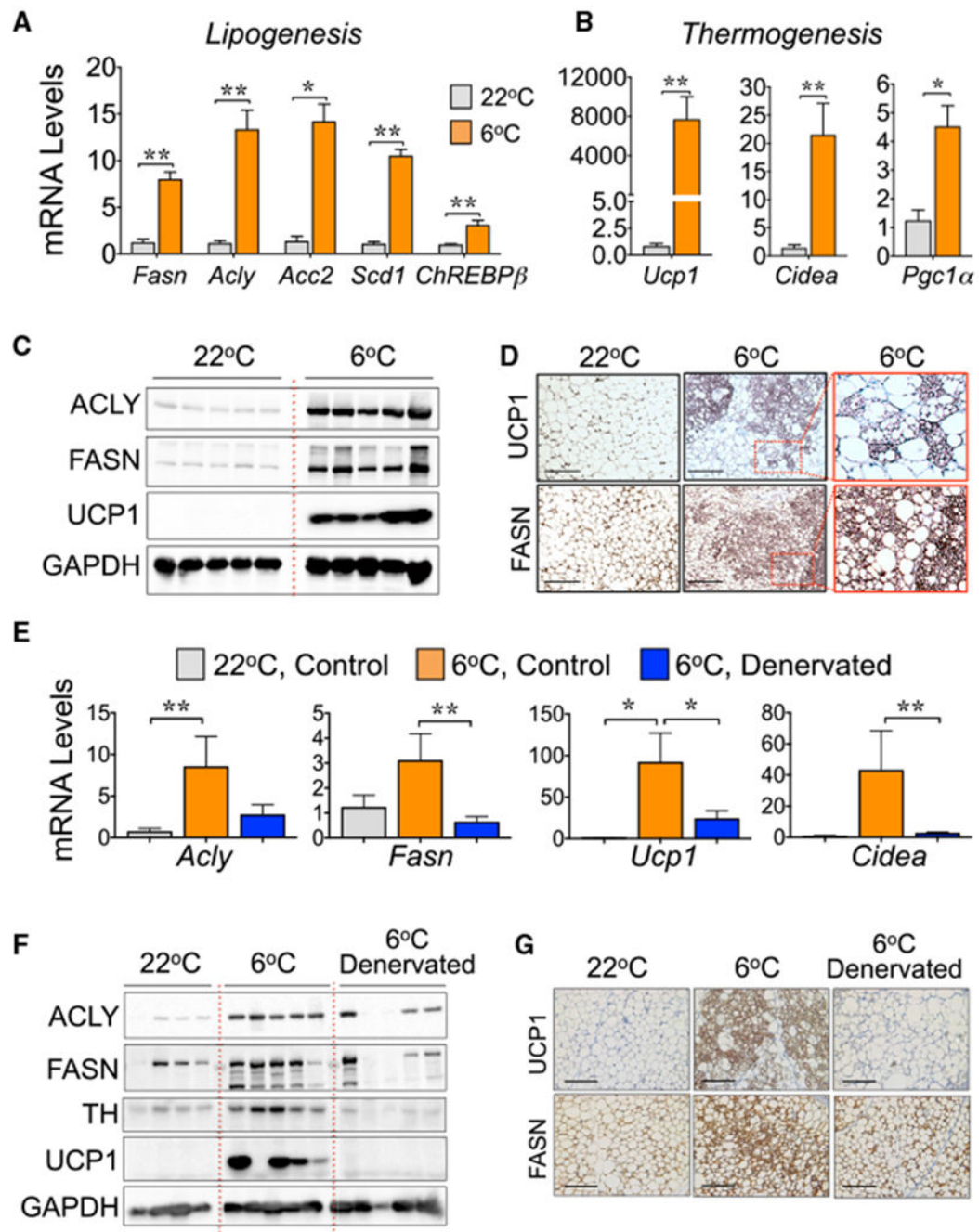- TR and β3-AR act cooperatively on UCP1, while TR promotes DNL without β3-AR signaling

Figure 1. Cold-Stimulated Sympathetic Drive Enhances DNL Gene Expressions along with the Thermogenic Program in WAT

(A) qRT-PCR depicting enhanced DNL gene expression in sWAT from male mice housed at 22°C or 6°C for 2 weeks.

(B) qRT-PCR showing enhanced thermogenic gene expression in sWAT from mice housed at 6°C. qRT-PCR was performed for the quantification of indicated mRNA expressions in sWAT from cold-exposed wild-type mice.

(C) Western blots of sWAT lysates from mice housed at 22°C or 6°C for 2 weeks, depicting enhanced expression of ACLY, FASN, UCP1, and GAPDH protein levels in cold-exposed mice. GAPDH was used as loading control.

(D) Immunohistochemistry (IHC) for the detection of UCP1 or FASN content in sWAT from mice housed at 22°C or 6°C for 2 weeks. Scale bar, 100 μm. Graphs show the means ± SEMs. n = 12 mice per group.

(E) Adipose sympathetic denervation inhibits cold-induced adipose DNL gene expressions. qRT-PCR was performed to quantify *Acly*, *Fasn*, *Ucp1*, and *Cidea* mRNA expression levels in sWAT from control mice kept at room temperature (22°C), control mice cold exposed at 6°C for 1 week, and 6-OHDA-denervated mice cold exposed at 6°C for 1 week.

(F) Western blots to detect ACLY, FASN, TH, UCP1, and GAPDH (loading control) protein levels in sWAT from vehicle-injected control mice kept at 22°C or 6°C for 1 week and chemically denervated mice exposed to cold (6°C) for 1 week.

(G) Representative IHC analysis for the detection of UCP1 and FASN protein in sWAT from vehicle-injected and chemically denervated mice cold exposed at 6°C for 1 week. Scale bar, 100 μm.

Graphs show the means ± SEMs. n = 6–8 mice per group. *p < 0.05 and **p < 0.01 by Mann-Whitney *U* test (A and B) or by 1-way ANOVA, followed by Tukey's post hoc test (E).
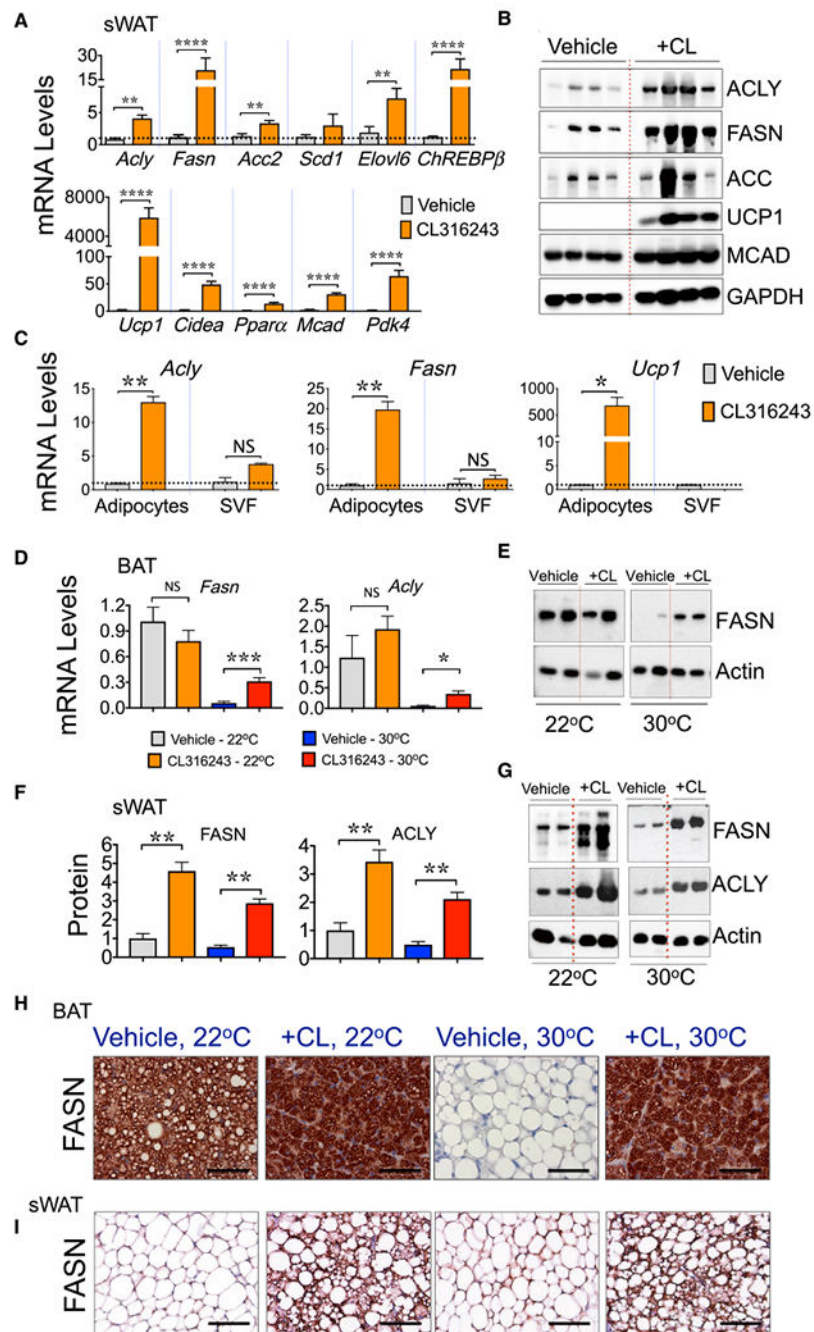
Figure 2. β3-Adrenergic Receptor (β3-AR) Agonist CL316243 Treatment Rescues the Adipose DNL Genes in Thermoneutral Mice

(A) qRT-PCR was performed for quantification of the indicated genes in sWAT depot from wild-type male mice housed at 22°C and treated with vehicle or with CL316243 for 6 days.

(B) Western blots of sWAT lysates from vehicle-treated and CL316243-treated mice depicting enhanced expression of FASN, ACC, ACLY, MCAD, and UCP1 proteins in CL-treated mice. GAPDH was used as loading control.

(C) β3-AR activation promotes DNL in adipocytes. qRT-PCR to quantify *Acly, Fasn, or Ucp1* mRNA expressions in adipocytes or in stromal vascular fraction (SVF) isolated from the sWAT of mice treated or not treated with CL316243 for 6 days.

(D–G) CL316243 treatment rescues the adipose DNL genes in thermoneutral mice. Adipose DNL is suppressed when SNS outflow and β3-AR activation in AT are negligible. (D) qRT-PCR to quantify *Fasn* and *Acly* mRNA levels in BAT from mice housed at 22°C or 30°C for 5 weeks and then treated or not treated with CL316243 for 6 days. Immunoblot depicting FASN protein levels in BAT(E) or sWAT (G) from mice housed at 22°C or 30°C treated with vehicle or with CL316243.

(F) FASN and ACLY protein levels were quantified by densitometry from the immunoblot data shown in (G).

(H and I) CL316243 treatment restores adipose DNL in thermoneutral mice. IHC to detect FASN in BAT (H) and sWAT (I) from mice kept at 22°C or 30°C and treated or not treated with CL316243 for 6 days. Scale bar, 100 μm.

Graphs show the means ± SEMs. n = 5–6 mice per group. *p < 0.05, **p < 0.01, ***p < 0.001, and ****p < 0.0001 by Mann-Whitney *U* test.
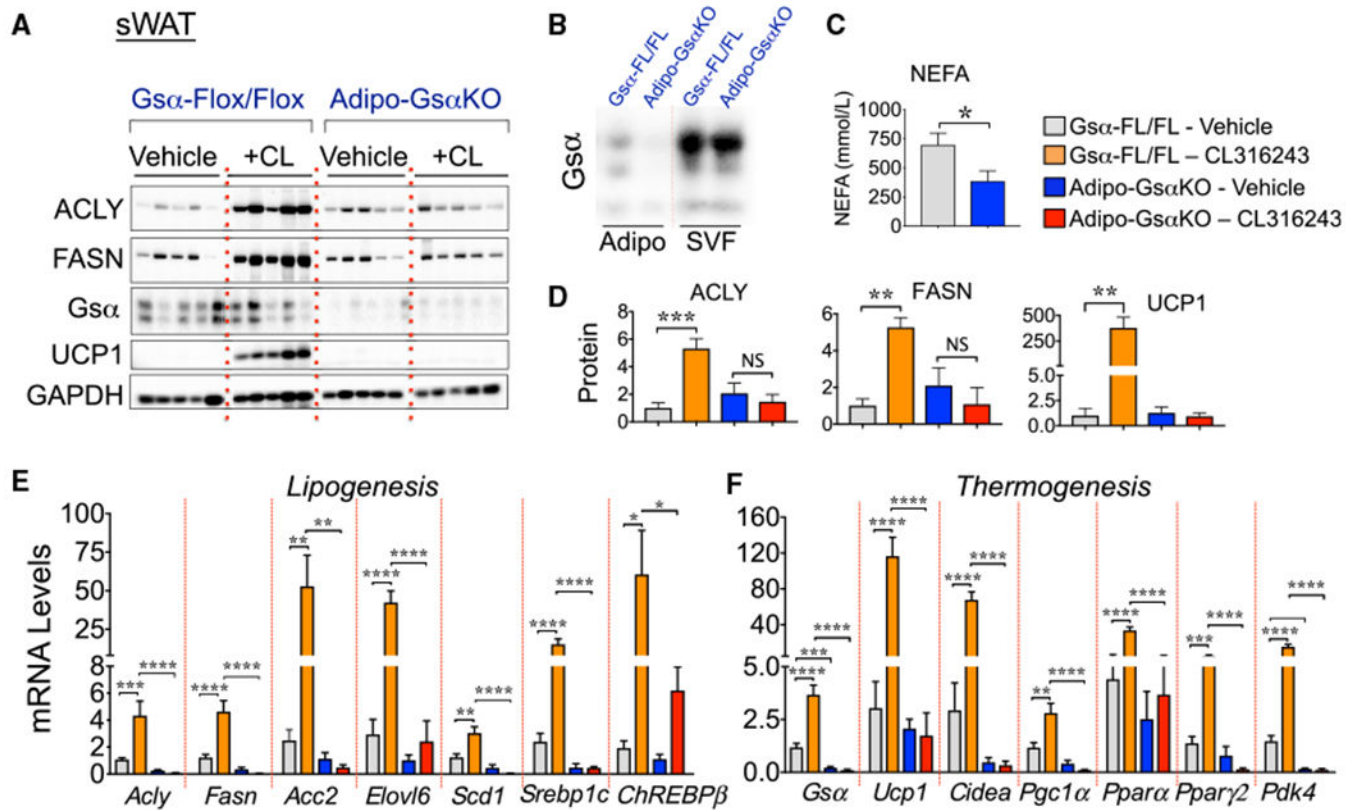
Figure 3. The cAMP Production in Adipocytes Is Required for β-AR-Induced Lipogenic Gene Expression in Swat

(A) Gsα-protein inactivation in adipocytes strongly inhibits the β3-mediated stimulation of DNL and induction of browning in sWAT. Depicted are representative western blots for lipogenic (ACLY and FASN) and thermogenic protein (UCP1) expression in sWAT from Gsα-Flox/Flox control and adipocyte-specific GsαKO mice (Adipo-GsαKO) treated with vehicle or with CL316243 for 6 days. GAPDH was used as loading control.

(B) Isolated adipocytes (Adipo) and stromal vascular fractions (SVFs) from Gsα-Flox/Flox or Adipo-GsαKO mice were immunoblotted for Gsα protein.

(C) The effect of adipocyte Gsα inactivation on circulating non-esterified fatty acids (NEFAs) is depicted. $*p < 0.05$ by Student's t test.

(D) Quantifications of proteins from the western blots depicted in (A).

(E and F) qRT-PCR analysis to quantify lipogenic (E) and thermogenic (F) gene expressions in sWAT from Gsα-Flox/Flox control and Adipo-GsαKO mice treated or not treated with CL316243.

Graphs show the means ± SEMs. n = 8 mice per group.

(D–F) $*p < 0.05$, $**p < 0.01$, $***p < 0.001$, and $****p < 0.0001$ by 1-way ANOVA, followed by Tukey's post hoc group comparisons.
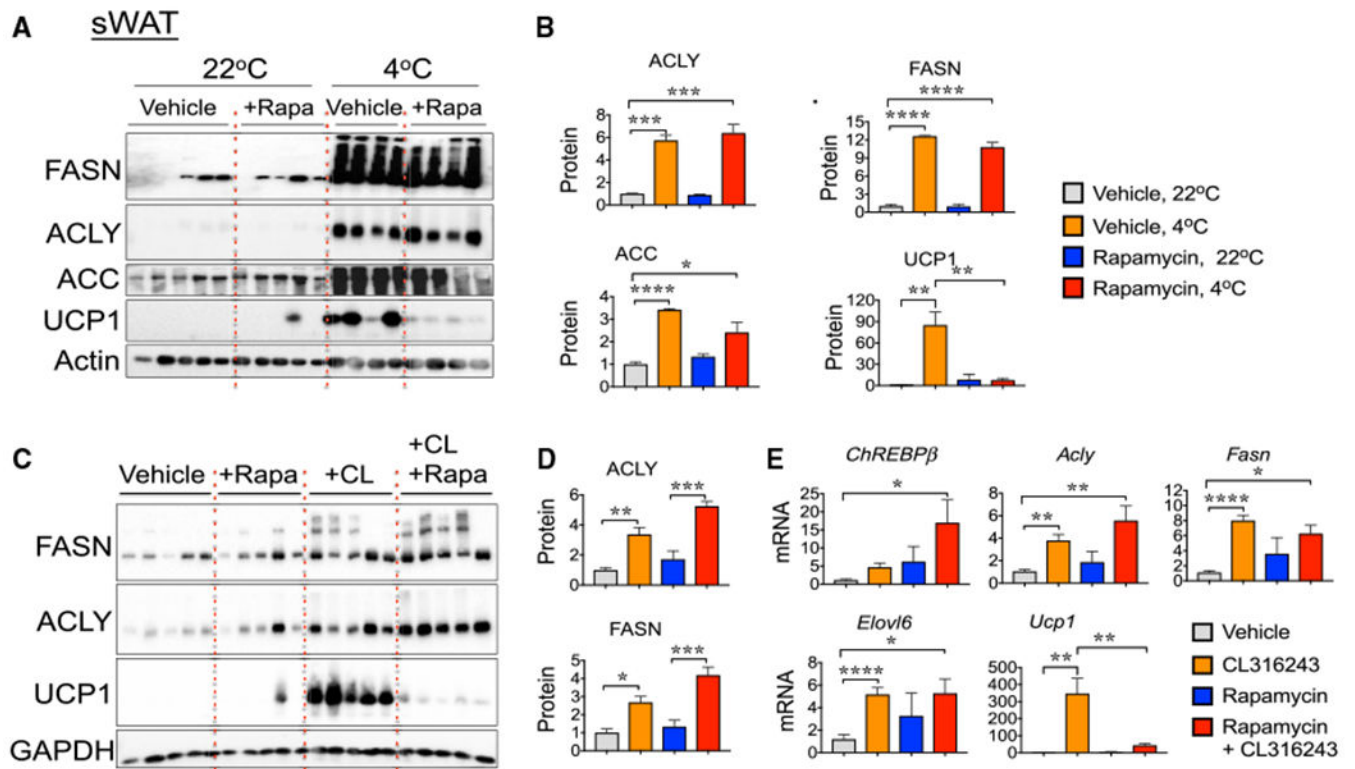
See also Figures S1 and S2.

Figure 4. Rapamycin Treatment Fails to Block the β3-AR-Stimulated DNL Gene Expression in WAT

(A) Rapamycin treatment inhibits cold-induced UCP1 expression, but not the DNL gene expression in sWAT. Western blots for the detection of DNL (FASN, ACLY, and ACC) and thermogenic (UCP1) proteins and actin (loading control) in sWAT from control mice (22°C) and mice exposed to 4°C for 1 week, treated with vehicle or rapamycin.

(B) Quantification from protein bands depicted in western blots from (A).

(C) Representative western blots to detect FASN, ACLY, UCP1, and GAPDH (loading control) proteins in sWAT from control and CL316243-treated mice, cotreated or not with rapamycin.

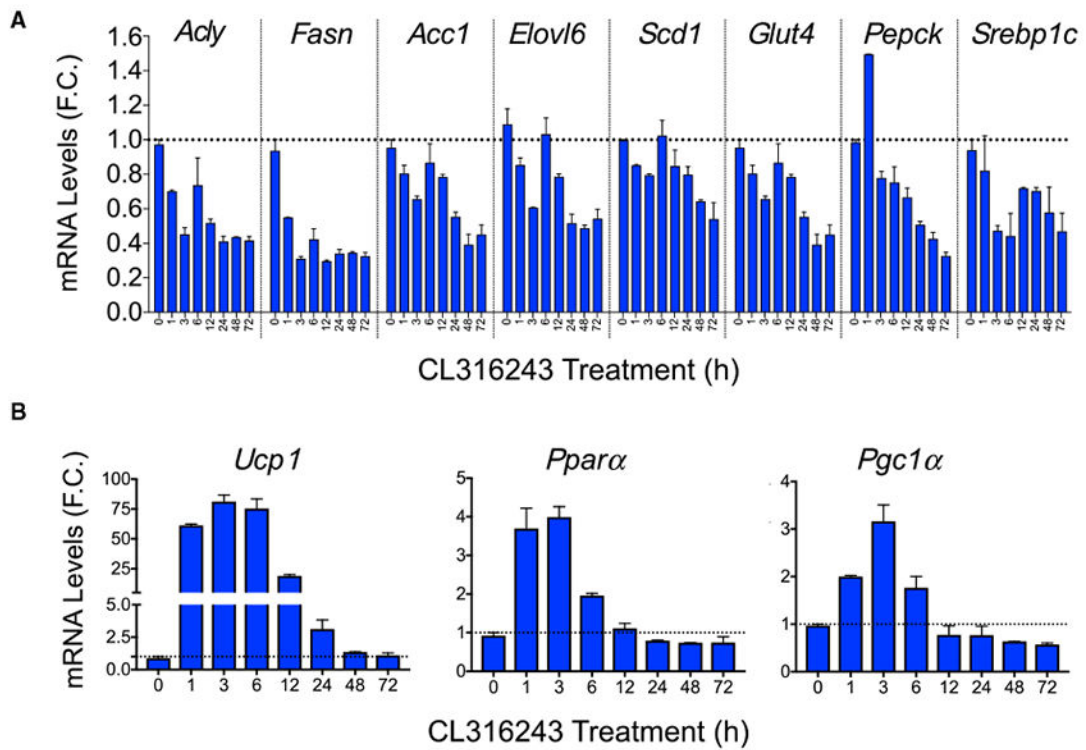(D) Quantification of protein bands shown in western blots from (C).

(E) qRT-PCR analysis of indicated DNL and thermogenic gene expression in sWAT from CL-treated mice, with or without rapamycin.

Graphs show the means ± SEMs. n = 6–8 mice per group.

(B, D, and E) *p < 0.05, **p < 0.01, ***p < 0.001, and ****p < 0.0001 by 1-way ANOVA, followed by Tukey's test for group comparisons.

See also Figure S3.

3T3-L1 Adipocytes
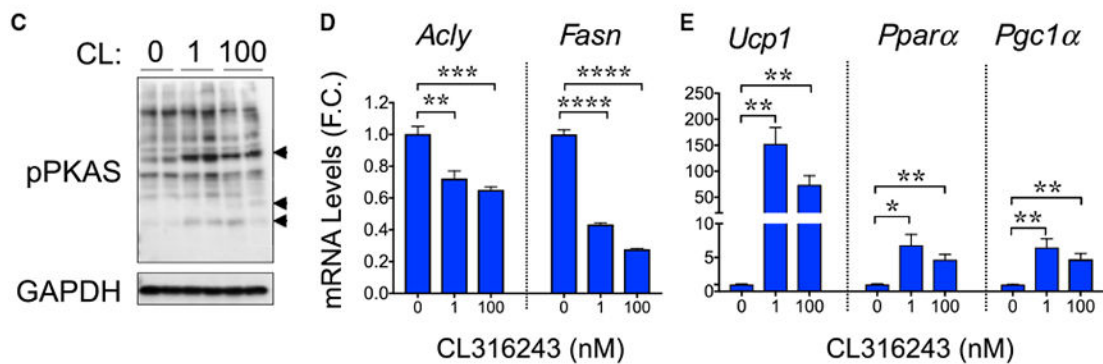

Primary Adipocytes

Figure 5. CL316243 Treatment *In Vitro* Failed to Induce DNL Gene Expression in Cultured Adipocytes

(A and B) qRT-PCR analysis of DNL (A) and thermogenic (B) gene expression in 3T3-L1 adipocytes (day 7 post-differentiation) treated with CL316243 (100 nM) for the indicated time points.

(C–E) Western blots for the detection of phospho-PKA substrates and GAPDH (loading control) protein levels in cultured primary adipocytes treated or not treated with different doses (0,1, and 100 nM) of CL316243 for 6 h (C). Also depicted are qRT-PCR quantifications to determine the expression levels of *Fasn* and *Adly* (D) and *Ucp1, Ppara*

and *Pgc1a* (E) mRNA in cultured primary adipocytes treated with indicated doses of CL316243 for 6 h.

Graphs show the means ± SEMs. n = 3 determinations. *p < 0.05, **p < 0.01, ***p < 0.001, and ****p < 0.0001.
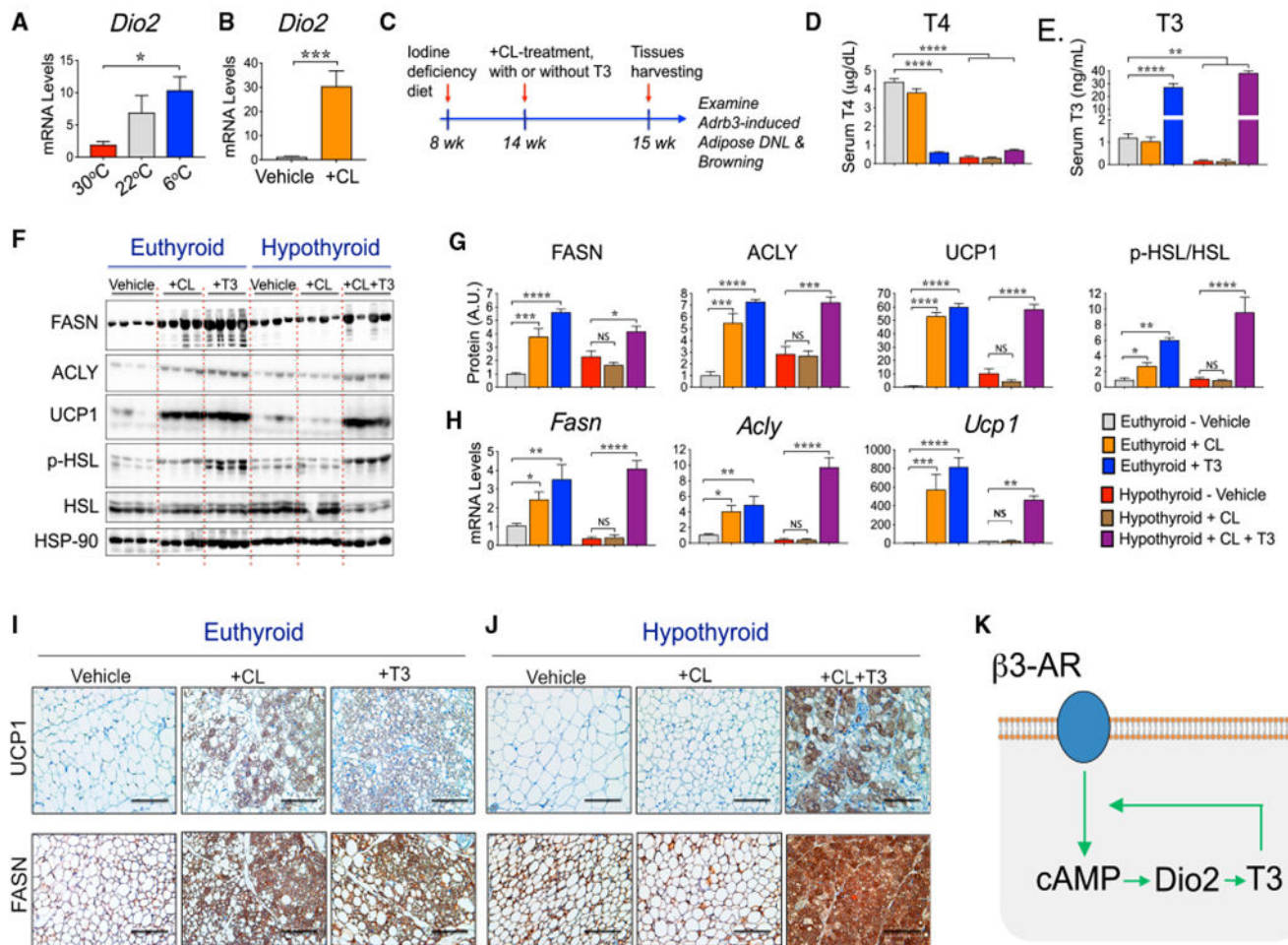
Figure 6. Thyroid Hormone Signaling Is Essential for β3-AR-induced DNL in Adipocytes

(A and B) Cold stimulus and CL316243 treatment enhance the expression levels of T3-producing enzyme iodothyronine deiodinase-2 (*Dio2*) in sWAT. Mice were housed at 30°C, 22°C for 8 weeks, or exposed to 6°C for 2 weeks (A) or housed at 22°C and treated with vehicle or with CL316243 for 6 days (B). *Dio2* mRNA levels in sWAT were then quantified by qRT-PCR.

(C) Wild-type mice were maintained on a control diet or iodine-deficient + PTU diet to inhibit thyroid hormone production. Mice were then treated or not treated with CL316243 to evaluate adipose β3-AR signaling in hypothyroid mice. Depicted is the diagram representing the experimental design.

(D and E) Iodine-deficient + PTU diet feeding strongly reduces the circulating levels of T4 (D) and T3 (E).

(F) Representative western blots to detect FASN, ACLY, UCP1, HSL, phospho-HSL, and HSP-90 (loading control) proteins in sWAT from euthyroid and hypothyroid mice treated with vehicle or with CL316243 or T3, as indicated.

(G) Quantification from protein bands depicted in western blots from (F).

(H) qRT-PCR quantifications to determine the expression levels of *Fasn, Acly*, and *Ucp1* mRNAs in sWAT from euthyroid and hypothyroid mice treated or not treated with the indicated agonists.

(I and J) Representative IHC analyses for the detection of UCP1 and FASN proteins in sWAT from euthyroid mice (I) or hypothyroid mice (J), treated or not treated with the indicated agonist. Scale bar, 100 μm.

(K) Proposed model depicting the feedforward cycle whereby cAMP and T3 amplify each other's activity.

Graphs show the means ± SEMs. n = 5 mice per group. In (A) and (D)–(H), *p < 0.05, **p < 0.01, ***p < 0.001, and ****p < 0.0001 by 1-way ANOVA, followed by post hoc group comparisons. In (B), *p < 0.05 by Student's t test. See also Figure S4.
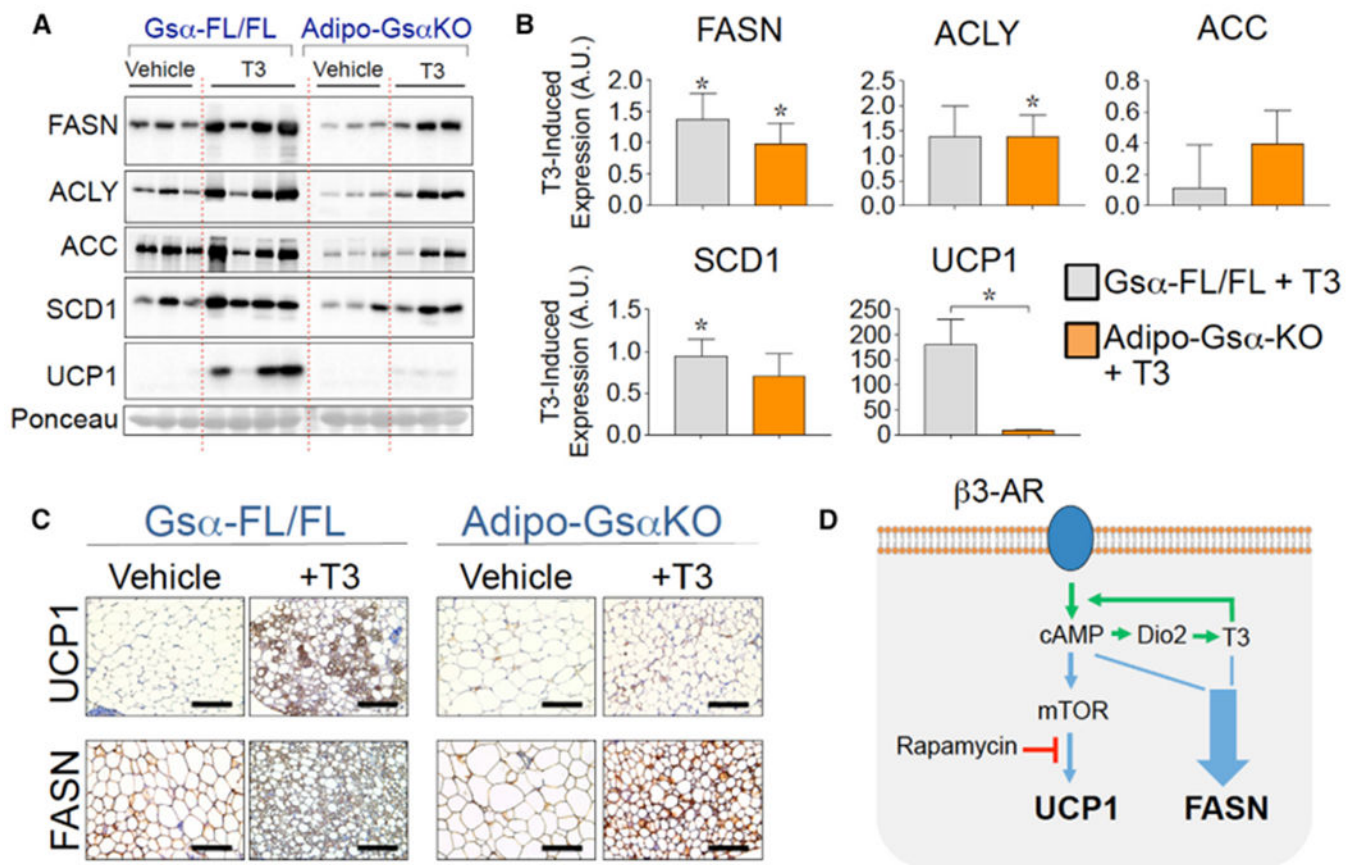
Figure 7. Triiodothyronine (T3) Treatment Partially Restores DNL in Adipocytes without cAMP

(A) Representative western blots for lipogenic (FASN, ACLY, ACC, and SCD1) and thermogenic protein (UCP1) expression in sWAT from Gsα-Flox/Flox control and Adipo-GsαKO male mice treated with vehicle or with T3 for 10 days. Nitrocellulose membrane was also stained with Ponceau S to confirm the equal loading of total protein.

(B) Quantification of protein bands from western blots depicted in (A). Shown are the incremental increases in FASN, ACLY, ACC, SCD1, and UCP1 proteins due to T3 treatment over those in the respective vehicle lanes. Graphs depict the means ± SEMs. n = 3–4 mice per group. *$p < 0.05$.

(C) Representative IHC analyses for the detection of UCP1 and FASN proteins in sWAT from Gsα-Flox/Flox control and Adipo-GsαKO mice treated with vehicle or with T3 for 10 days. Scale bar, 100 μm.

(D) Proposed model shows how β3-AR and thyroid hormone signal integration controls thermogenesis (UCP1) and *de novo* lipogenesis (FASN) in adipocytes. Both thermogenesis and T3-induced DNL are driven by β3-AR signaling intrinsically.

See also Figures S5 and S6.

KEY RESOURCES TABLE

REAGENT or RESOURCE	SOURCE	IDENTIFIER
Antibodies		
Anti-Fatty Acid Synthase, Clone 23	BD Bioscience	Cat# 610963; RRID:AB_398276
Anti-Fatty Acid Synthase	Abcam	Cat# ab22759; RRID:AB_732316
Anti-UCP1	Abcam	Cat# ab10983; RRID:AB_2241462
Anti-Tyrosine Hydroxylase	Abcam	Cat# ab75875; RRID:AB_1310786
Anti-Deiodinase-2	Abcam	Cat# ab77779; RRID:AB_1951738
Anti-ACLY	Proteintech	Cat# 15421-1-AP; RRID:AB_2223741
Anti-ACC	Cell Signaling Technology	Cat# 3662; RRID:AB_2219400
Anti-SCD1	Cell Signaling Technology	Cat# 2794; RRID:AB_2183099
Anti-pHSL(Ser563)	Cell Signaling Technology	Cat# 4139; RRID:AB_2135495
Anti-phospho PKA substrate (RRXS*/T*)	Cell Signaling Technology	Cat# 9624; RRID:AB_331817
Anti-pCREB(Ser133)	Cell Signaling Technology	Cat# 9198; RRID:AB_2561044
Anti-GAPDH	Cell Signaling Technology	Cat# 2118; RRID:AB_561053
Anti-MCAD	Santa Cruz Biotechnology	Cat# sc-365109; RRID:AB_10709904
Anti-HSP-90	Santa Cruz Biotechnology	Cat# sc-7947; RRID:AB_2121235
Anti-β-Actin	Sigma-Aldrich	Cat# A2228; RRID:AB_476697
Anti-Rabbit IgG antibody, HRP-conjugated	Millipore	Cat# AP307P; RRID:AB_11212848
Anti-Mouse IgG antibody HRP-conjugated	Millipore	Cat# AP308P, RRID:AB_11215796
Anti-Gsα	Li et al., 2016	N/A
Chemicals, Peptides, and Recombinant Proteins		
Tamoxifen	Sigma-Aldrich	Cat# T5648
CL 316,243	Sigma-Aldrich	Cat# C5976
6-Hydroxydopamine hydrochloride (6-OHDA)	Sigma-Aldrich	Cat# H4381
Rapamycin	LC Laboratories	Cat# R-5000
Ethanol	American Bio	Cat# AB00515
Polyethylene glycol 300 (PEG 300)	Hampton Research	Cat# HR2–517
Tween 80	Sigma-Aldrich	Cat# P1754
Tween 20	Sigma Aldrich	Cat# P1379
3,3′,5-Triiodo-L-thyronine (T3)	Cayman Chemicals	Cat# 16028
Iodine deficient diet (0.15% PTU)	ENVIGO	Cat# TD.95125
Ingredient matched control diet	ENVIGO	Cat# TD.97350
Bovine serum albumin (fatty acid free)	Sigma-Aldrich	Cat# A8806
D-(+)-Glucose	Sigma-Aldrich	Cat# G8270
Sodium acetate	Sigma-Aldrich	Cat# S5636
Sodium pyruvate	GIBCO	Cat# 11360070
L-Glutamine	GIBCO	Cat# 25030081
[^{14}C]-U-Glucose	Perkin Elmer	Cat# NEC042X250UC

REAGENT or RESOURCE	SOURCE	IDENTIFIER
DMEM/F-12	GIBCO	Cat# 11330032
Penicilin/Streptomycin	GIBCO	Cat# 15140122
Normocin	Invivogen	Cat# ant-nr-1
Fetal bovine serum (FBS)	Atlanta Biologicals	Cat# S11550
Phosphate-buffered saline (PBS)	GIBCO	Cat# 14190144
Dibutyryl-cAMP	Tocris Bioscience	Cat# 1141
QIAzol Lysis Reagent	QIAGEN	Cat# 79306
Critical Commercial Assays		
Serum total T3	Calbiotech, Inc	Cat# T3043T-100
Serum total T4	Calbiotech, Inc	Cat# T4044T-100
Serum NEFA	Fujifilm Wako Diagnostics	Cat# 999-34691
Free Glycerol Reagent	Sigma-Aldrich	Cat# F6428
Enhanced Chemiluminescent Substrate kit	Perkin Elmer	Cat# NEL104001EA
iScript™ cDNA Synthesis Kit	Bio-Rad Laboratories	Cat# 1708891
iTaq Universal SYBR® Green Supermix	Bio-Rad Laboratories	Cat# 1725121
Experimental Models: Cell Lines		
3T3-L1 cell line	ATCC	Cat# CL-173™; RRID:CVCL_0123
Experimental Models: Organisms/Strains		
Mouse: C57BL/6J	The Jackson Laboratory	Stock# 000664; RRID: IMSR_JAX:000664
Mouse: *Gsa-Flox/Flox*	Li et al., 2016	N/A
Mouse: *Adipoq-cre: B6;FVB-Tg*$^{(Adipoq-cre)1Evdr/J}$	The Jackson Laboratory	Stock# 010803; RRID: IMSR_JAX:010803
Mouse: Adipo-GsαKO	Li et al., 2016	N/A
Mouse: *Adipo-Cre: B6.129-Tg*$^{(Adipoq-cre/Esr1 *)1Evdr/J}$	The Jackson Laboratory	Stock# JAX:024671, RRID:IMSR_JAX:024671
Mouse: *iAdipo-GsαKO, inducible*	This paper	N/A
Oligonucleotides		
See Table S1 for primers used for qRT-PCR	This paper	N/A
Software and Algorithms		
GraphPad Prism 8	GraphPad	GraphPad Software, Inc
Image Lab 5 Analysis Software	Bio-Rad Laboratories	Iten# 1709690
ImageJ	ImageJ	ImageJ.nih.gov
Other		
ChemiDoc™ XRS+ Imaging System	Bio-Rad Laboratories	Model# 1708265
Leica DM2500 LED optical microscope	Leica Microsystems	Model# DM2500 LED
Leica MC170 HD camera	Leica Microsystems	Model# MC170 HD